PROCEEDINGS OF THE YEREVAN STATE UNIVERSITY

Physical and Mathematical Sciences 2017, **51**(1), p. 101–104

P h y s i c s

PHASE-CONTRAST IMAGING BASED ON THREE-BLOCK FRESNEL ZONE PLATE INTERFEROMETERS USING HARD X-RAY LABORATORY SOURCES

L. A. HAROUTUNYAN *

Chair of Solid State Physics YSU, Armenia

The earlier represented three-block Fresnel Zone Plate interferometer based hard X-ray phase-contrast imaging setup designed for the initial plane wave radiation has been adapted to the laboratory sources of radiation. The limited distance between the source and the interferometer as well as the finite size of the source and the limited degree of monochromaticity of the illumination have been taken into account. It was shown that the decrease of the spatial coherency of the initial radiation does not worsen, and even improves the quality of the phase-contrast imaging, by suppressing the distortions caused by the X-ray diffraction at the edges of the Fresnel zone plates and the knifes of the interferometer.

***Keywords*:** X-ray optics, Fresnel zone plate, phase-contrast.

Introduction. The first experimental set-ups of hard X-ray phase-contrast imaging by the interferometric method are based on the use of Bonze-Hart three-block interferometer with the Laue diffraction geometry (LLL-interferometer) [1, 2]. The phase object under investigation (the object from light elements such as soft biological tissues), is allocated across the path of one of the propagation channels of the interferometer - of the object wave. This results in a corresponding phase modulation of the object wave, which causes the bending of the registered interference fringes [3]. The restoration of the phase shift distribution from the registered interference pattern is carried out by special algorithms such as the Fourier transform method [4] and the fringe scanning method [5]. The interferometer operates in the amplitude-division mode, with the equal lengths of trajectories in both channels of propagation. As a result, it does not impose strong requirements to the coherency of the initial X-ray radiation. Note that the interferometer has been implemented experimentally in the 60s of the last century with the hard X-ray sources of that time.

In the last couple of decades the development of the fabrication technologies of the Fresnel Zone Plates (FZP) has enabled the use of the FZP in the X-ray interferometers. Such combination of focusing optics and interferometry makes the realization of the phase-contrast imaging with optical magnification possible. The schemes of the interferometric method phase-contrast imaging, based on the interferometers with two FZP located both on the same plane [6] and shifted relative to each other along the optical axis [7, 8], are already implemented. In these schemes, however, the interferometers operate in the wave front-division mode and impose strong requirements to the coherency of initial radiation. However, these requirements are met at the modern sources of the synchrotron radiation.

* E-mail: levhar@ysu.am, levon.har@gmail.com

Another scheme of the phase-contrast imaging based on the three-block X-ray interferometer with FZP (Fig. 1, a) has also been presented [9]. The interferometer consists of three identical FZP with common optical axis and the distances between adjacent blocks equal to the doubled focal length of the FZP. The interference between the following two propagation channels is considered:

- the object wave: a wave passed through the first FZP and diffracted at the first order on the second and third FZP;
- the reference wave: a wave diffracted at the first order on the first and second FZP and passed through the third FZP.

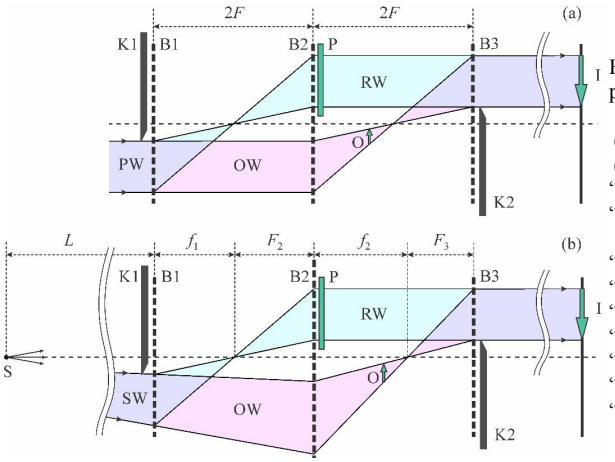

Fig. 1. Schematic diagrams of phase contrast imaging facilities for initial:
(a) plane wave;
(b) spherical wave.
"S" the spherical wave source;
"B1", "B2", "B3" interferometer blocks;
"P" phase shifter;
"O" tested phase object;
"I" image of the test object;
"OW" object wave;
"RW" reference wave;
"PW" initial plain wave;
"SW" initial spherical wave.

The suppression of other "undesirable" channels of propagation is carried out by two knifes placed at the first and third FZP (Fig. 1, a) and by sufficient distance between the third FZP and the detector. The spatial separation of the interfering beams, which is important in phase-contrast imaging, is also caused by the same knifes. The phase shifter is placed at the path of the reference wave after the second FZP, and the test object in the path of the object wave before its focusing, so as its sharp image due to the diffraction of object wave in third FZP would be formed strictly on the detector. Interferometer operates in the amplitude-division mode with the equal lengths of trajectories in both propagation channels, which softens the requirements for the spatial and temporal coherence of the initial radiation. This circumstance, as well as the geometrical narrowing of the object wave before its falling on the test object (it is important for the low-power radiation sources) are the basis for considering the feasibility of using the laboratory X-ray sources with this device.

Phase-Contrast Imaging with the Use of Hard X-Ray Laboratory Sources. A modified version of above presented phase-contrast imaging device wherein the initial plane wave is replaced by the spherical one shown in Fig. 1, b. The values of the basic parameters of the device must satisfy the following equations:

$$\begin{gathered} F_2 = f_1 = \frac{L}{L-F_1}F_1, \\ f_2 = \frac{L+F_1}{L-F_1}F_1, \qquad R_2 = \frac{L+F_1}{L-F_1}R_1, \\ F_3 = F_1, \quad R_3 = R_1, \end{gathered} \tag{1}$$

where F_i and R_i are the first-order focal length and the radius of the i-th FZP respectively, and L is the distance of the radiation point-source situated on the optical axis from the first block of the interferometer.

Interferometer still operates in the amplitude-division mode, but the lengths of the trajectories of two propagation channels are now differ by $\Delta l = \lambda N \gamma$, where λ is the X-ray wavelength, $\gamma = 2F_1/(L-F_1)$. The requirement for a degree of monochromaticity of initial radiation corresponding to this paths difference is $\Delta\lambda/\lambda \leq (2N_1\gamma)^{-1}$, which at $L \geq 5F_1$ does not exceed the requirement of the FZP at radiation focusing.

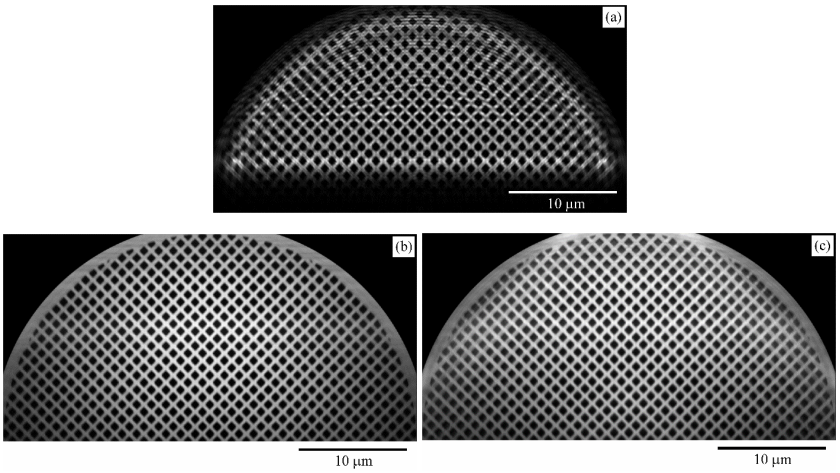

Fig. 2. Numerical simulation of phase-contrast imaging with the facilities for initial spherical wave, using: (a) a monochromatic point source; (b) monochromatic finite size source; (c) quasi-monochromatic finite size source of radiation.

The numerically simulated interference pattern of the presented device for the monochromatic point-source of the radiation is represented in Fig. 2, a. As the test-object, a silicon wafer with the etched strips forming a rectangular grid with period of 956 *nm* is considered. The width and depth of the strips are 383 *nm* and 3.06 μm respectively. The numerical values of other significant parameters used in the computing are given below. The X-ray wavelength $\lambda = 1.54$ *Å* (characteristic line CuK_{α_1}), the radii and focal lengths of the used FZP: $R_1 = R_3 = 153\ \mu m, R_2 = 187\mu m$, $F_1 = F_3 = 0.2\ cm$ and $F_2 = 22.2\ cm$ (the widths of outermost zones are: $\Delta R_1 = \Delta R_3 = 100.7\ nm$, $\Delta R_2 = 91.5\ nm$). The depth of etching of zone structure of the silicon FZP is $4.07\mu m$, which for the considered wavelength of radiation results in the 13.6% focusing efficiency for the first order diffraction (the absorption of radiation in the substrate is not taken into account). The optical magnification coefficient is $G = 8$. The phase shift of the phase shifter is set in the antiphase with the phase shift of the test object in the absence of strips. The numerical calculations are based on the integration of the Helmholtz equation by two-dimensional Fourier transform method [10]. Objects at the path of the X-rays are considered to be flat and described by the complex amplitude transmission coefficients, which are the functions of two transverse coordinates to the optical axis [11, 12]. Besides a clear mapping of the test object structure, there are noticeable distortions in the registered interference pattern in the form of horizontal stripes and semirings. The author believes that they are the result of the diffraction of the X-ray beams at the edges of the FZP and the knifes. Similar distortions are also noticeable in the case of the initial plane wave [9], with the use of the device represented in Fig. 1, a.

The similar computations have been also carried out for the finite size sources with mutually-independent radiating points both for the monochromatic (Fig. 2, b) and the quasi-monochromatic illumination. The source size is $180 \times 180\ \mu m^2$ and the degree of monochromaticity in the case of Fig. 2, c: $\Delta\lambda/\lambda = 2 \cdot 10^{-3}$, which are completely accessible in the

laboratory conditions. As can be seen from the computations, the limited spatial coherence of initial radiation (the finite dimension of the source), does not worsen, but rather improves the quality of mapping by suppressing the diffraction distortions, which are present in the cases of point sources (Fig. 2, a) and the initial plane wave [9]. The increase in the imaged area of the test object is due to the inclination of rays formed by the areas of the source remote from its central part.

Conclusion. The presented here three block interferometer can be applied for hard X-ray phase-contrast imaging using laboratory sources of radiation. The low spatial coherence, which is inherent in laboratory sources, does not worsen and even improves the quality of mapping by suppressing the unwanted diffraction distortions, which are present in the case of a point source and initial plane wave. The geometric restriction of the object wave before its incidence on the tested object results in a "gain" in intensity, which is especially important for laboratory sources of radiation.

Received 22.12.2016

REFERENCES

1. **Bonse U., Hart M.** An X-ray Interferometer. // Appl. Phys. Lett., 1965, v. 6, p. 155.
2. **Bonse U., Hart M.** Principles and Design of Laue-Case X-ray Interferometers. // Z. Physik., 1965, v. 188, p. 154.
3. **Momose A.** Demonstration of Phase-Contrast X-ray Computed Tomography Using an X-ray Interferometer. // Nucl. Instr. Meth. A, 1995, v. 352, p. 622.
4. **Takeda M., Ina H., Kobayashi S.** Fourier-Transform Method of Fringe-Pattern Analysis for Computer-Based Topography and Interferometry. // J. Opt. Soc. Am., 1982, v. 72, p. 156.
5. **Bruning J.H., Herriott D.R., Gallagher J.E., Rosenfeld D.P., White A.D., Brangaccio D.J.** Digital Wavefront Measuring Interferometer for Testing Optical Surfaces and Lenses. // Appl. Opt., 1974, v. 13, p. 2693.
6. **Koyama T., Saikubo A., Shimose K., Hayashi K., Nakagawa A.** et al. Hard X-ray Micro-Interferometer for High-Spatial-Resolution Phase Measurement. IPAP Conf. Ser. Proc. 8th Int. Conf. // X-ray Microscopy, 2006, v. 7, p. 389.
7. **Wilhein T., Kaulich B., Susini J.** Two Zone Plate Interference Contrast Microscopy at 4 *keV* Photon Energy. // Opt. Commun., 2001, v. 193, p. 19.
8. **Koyama T., Tsuji T., Yoshida K., Takano H., Tsusaka Y., Kagoshima Y.** Hard X-ray Nano-Interferometer and Its Application to High-Spatial-Resolution Phase Tomography. // Jpn. J. Appl. Phys., 2006, v. 45, p. L1159.
9. **Haroutunyan L.A.** X-ray Phase Contrast Imaging with Optical Magnification Using Three-Block Interferometer with Bi-Level Fresnel Zone Plates. // J. Contem. Phys. (Armenian Ac. Sci.), 2016, v. 51, p. 284.
10. **Goodman J.W.** Introduction to Fourier Optics. NY: McGraw-Hill, 1996.
11. **Kohn V.G., Snigireva I.I., Snigirev A.** Numerical Modeling of Optical Properties of a System of Two Zone Plates for Focusing Hard Synchrotron Radiation. // Crystallography Reports, 2006, v. 51, p. S4.
12. **Kohnand V.G., Orlov M.A.** Computer Simulation of the Zernike Phase Contrast in Hard X-ray Radiation Using Refractive Lenses and Zone Plates. // J. Surface Investigation, 2010, v. 4, p. 941.